



ORIGINAL ARTICLE

Electrochemical synthesis of copper-arabinoxylan nanocomposite for applications as antimicrobial agent and CO₂ conversion catalyst



Almas Hamid ^a, Sajid Rashid Ahmad ^a, Mohammad Saeed Iqbal ^{b,*}, Iffat Naz ^{c,*},
Muhammad Zahid Qureshi ^{d,*}, Fozia Iram ^e

^a College of Earth & Environmental Sciences, University of the Punjab, Lahore 54600, Pakistan

^b Department of Chemistry, Forman Christian College, Lahore 54600, Pakistan

^c Department of Biology, Science Unit, Deanship of Educational Services, Qassim University, Buraidah 51452, Saudi Arabia

^d Department of Biochemistry, Science Unit, Deanship of Educational Services, Qassim University, Buraidah 51452, Saudi Arabia

^e Department of Chemistry, LCW University, Lahore 54600, Pakistan

Received 4 July 2022; accepted 13 November 2022

Available online 21 November 2022

KEYWORDS

Arabinoxylan;
Hemicelluloses;
Copper nanoparticles;
Green synthesis;
Antibacterial activity;
Catalytic activity

Abstract This study reports the electrochemical synthesis, antimicrobial and catalytic activity of copper-arabinoxylan nanocomposite. The synthesis was achieved without use of any hazardous reducing and stabilizing agent. The spherical copper nanoparticles (size approx. 40 nm) dispersed in the arabinoxylan matrix as they formed and got stabilized. In the absence of arabinoxylan the particles rapidly converted to copper oxide suggesting a high stability for the composite. Electrolysis was carried out with copper plate as the sacrificial anode, carbon rod as the cathode and sodium nitrate (1.00 % in 1 % arabinoxylan suspension) as an electrolyte. The copper nanoparticles dispersed in arabinoxylan were characterized by surface plasmon resonance spectroscopy, X-ray diffraction, electron microscopy and zeta potential measurements. The synthesized composite exhibited good antimicrobial activity against *P. aeruginosa*, *Staph. aureus* and *E. coli* and a catalytic activity in conversion of CO₂ to methanol.

© 2022 The Author(s). Published by Elsevier B.V. on behalf of King Saud University. This is an open access article under the CC BY-NC-ND license (<http://creativecommons.org/licenses/by-nc-nd/4.0/>).

* Corresponding authors.

E-mail addresses: almas209@yahoo.com (A. Hamid), sajidpu@yahoo.com (S. Rashid Ahmad), saeediq50@hotmail.com (M. Saeed Iqbal), I.Majid@qu.edu.sa (I. Naz), M.Qureshi@qu.edu.sa (M. Zahid Qureshi), fozia_iram@hotmail.com (F. Iram).

Peer review under responsibility of King Saud University.



1. Introduction

Copper nanoparticles (CuNPs) find use in electronics, catalysis, gas sensors, super conductors, environmental remediation and as antimicrobial agents (Akintelu et al., 2020; Ali et al., 2018; Gawande et al., 2016; Guo et al., 2016; Kumar et al., 2017a; Pant et al., 2017). One of the most exciting applications of CuNPs embedded in polymers is their use in the ink for printing nano-circuits, where the printed board is heated to 200–300 °C to burn off the polymer leaving the circuit behind (Numaga et al., 2020; Pant et al., 2017). For this, the polymer

must be degradable in this temperature range. Arabinoxylan (AX), being environmentally friendly material, offers a good opportunity for such an application (Iqbal et al., 2011; Akbar et al., 2012). Another important use of CuNPs is in purification of water, where the polymer carrying the particles must be biocompatible and biodegradable (Kruk et al., 2019; Morsi et al., 2017). Again, AX presents suitable properties for this application.

The CuNPs are known to exert prolonged antibacterial activity due to their large surface area and are less toxic to mammalian cells than in the ionic form (Rakhmetova et al., 2010). They produce reactive oxygen species, which cause lipid peroxidation, membrane disintegration and breakdown of genomic DNA (Majumdar et al., 2019). Gelatin-stabilized CuNPs have been reported to form cell filament and kill *E. coli* (Chatterjee et al., 2012).

Catalytic activity of copper in various organic reactions is well established (Nasrollahzadeh et al., 2015). Very few studies reporting catalytic activity of CuNPs in conversion of CO₂ to methanol can be found in literature. Hence, Cu-based catalysts continue to be a hot topic of research for production of methanol by hydrogenation of CO₂. CuNPs stabilized by reduced graphene oxide have been studied for CO₂ reduction to various species (Alves et al., 2015) and CuNPs supported on nanocrystalline ZnO have shown conversion of CO₂ to methanol at 450 °C (Ponce & Klabunde 2005). CuNPs produced by reduction of Cu₂O have also been reported to exert catalytic activity in conversion of CO₂ to methanol (Kas et al., 2014; Le et al., 2011). Similar study using citrate-stabilized CuNPs has also been reported (Dongare et al., 2021).

Several synthetic approaches have been adopted to synthesize stable CuNPs (Begletsova et al., 2018; El Bialy et al., 2020; Barrière et al., 2012; Benavente et al., 2013; Chiriac et al., 2016). Almost all of them employed expensive and hazardous reducing and stabilizing agents. The harsh chemicals and solvents employed during synthesis are difficult to remove and are ultimately released into the environment with detrimental consequences. Moreover, synthesis of CuNPs presents a great challenge as they are highly unstable (convert to CuO) and difficult to prepare in aqueous media. Hence, efforts are being focused on the development of environmentally friendly and cost-effective processes for the synthesis of stable CuNPs.

Keeping all these issues in view, the objectives of this work were set as: i) to synthesize CuNPs without the use of hazardous and non-biocompatible reducing and stabilizing agents; ii) to determine the antibacterial activity of the synthesized particles; iii) to determine the disinfection efficiency of polluted water and iv) to determine the catalytic activity of the particles for conversion of CO₂ to methanol.

Thus, in the present work electrochemical reduction has been used in the presence of AX to disperse the particles instantaneously in the polymer matrix and stabilize them. Studies have reported preparation of CuNPs by electrochemical reduction using various copper salts (Jain et al., 2019; Murtaza et al., 2019). Yet, to the best of our knowledge, no study has been reported involving the use of any hemicellulose as a dispersing and stabilizing agent. It was hypothesized that hemicelluloses such as AX can readily disperse and stabilize CuNPs as they are formed by electrochemical reduction without using any harmful and toxic reducing and stabilizing materials.

2. Materials and methods

2.1. Materials

Sodium nitrate (PubChem CID: 24268), roxithromycin (PubChem CID: 444037), Nutrient agar (PubChem CID: 71571511), nutrient broth and Luria broth were from Sigma-Aldrich, USA. Copper plate (99.99 %) was purchased from local market. Carbon rod was obtained from a dry battery cell

(LR20G R). Arabinoxylan, having an average molar mass of 3.17×10^6 Da, from *Plantago ovata* seed husk, was a gift from Dr. Shazma Massey of FC College Lahore (Massey et al., 2016). The bacterial strains used were: *P. aeruginosa* (ATCC 15442), *Staph. aureus* (ATCC 25923) and *E. coli* (ATCC 25922). Hydrogen (99.999 %), carbon dioxide (99.99 %) was from Matheson, USA. Nanopure® water was used throughout this work. All the chemicals were used without further purification.

2.2. Electrochemical synthesis of copper-arabinoxylan nanocomposite

AX (1.00 g) was dispersed in water (100 mL) by mechanical stirring to obtain a translucent suspension. To this, NaNO₃ (1.0 g) was added under stirring and labeled as electrolytic medium. The cell was set up in a 200-mL beaker using the copper plate (4 × 6 cm) as the anode and a carbon rod as the cathode. A variable DC power supply was connected to the electrodes and current was allowed to pass for 30 min under continuous stirring by a magnetic stirrer. The experiments were carried out at 1.5, 3.0, 4.5 V; the current was recorded to be ~5 A. The CuNPs formed and dispersed in AX matrix and the composite was isolated by centrifugation at 3000 rpm for 15 min and dried in a vacuum desiccator. The synthesis was repeated in triplicate at each voltage.

2.3. Characterization of copper-arabinoxylan nanocomposite

The surface plasmon resonance (SPR) spectra were recorded by suspending the prepared Cu-AX nano composites in acetone (1 w/v %) using Pharmaspec UV-1700 spectrophotometer (Shimadzu, Japan) in 200–800 nm range. FT-IR spectra of AX and the composite were recorded in the range 4000–500 cm⁻¹ by placing the sample on the ATR diamond crystal of the FT-IR spectrophotometer (IR-prestige-20 spectrophotometer, Shimadzu, Japan). The powder X-ray diffraction (pXRD) spectra were recorded by the D8 Discovery diffractometer (Bruker, Germany) using monochromatic Cu-K α radiation ($\lambda = 1.5406 \text{ \AA}$) operating at 40 kV and 30 mA. The data were collected in the range 10–80° 2 θ . The size of particles was calculated from the highest intensity peak in the XRD spectra by use of Debye–Scherrer equation ($D = 0.9\lambda/\beta\cos \theta$, where D is the crystal size, λ is the wavelength of X-ray, θ is the Bragg angle in radians, and β is the full width at half maximum of the peak in radians) (Scherrer, 1912). In order to record images by scanning electron microscopy (SEM) an ultrasonically dispersed suspension of the CuNPs in acetone was placed on a carbon coated grid and images were obtained by Nova NanoSEM 450 (FEI, Japan) at an accelerating voltage of 20 kV.

Zeta sizer NanoZS90 HPPS 5001 (Malvern, UK) was used to determine particle size and zeta potential (ζ) using a suspension of the composite in water (2 mg per 10 mL). For particle size determination, a disposable cuvette was filled with the sample and allowed to equilibrate for 2–3 min at 21 °C before the measurement. For ζ measurements, the capillary cell (DTS 1060) was flushed with water and filled with sample avoiding air bubbles in the capillary. These measurements were carried out as 10 replicates and average values were reported.

2.4. Antimicrobial activity of copper-arabinoxylan nanocomposite

Antibacterial activity of synthesized copper-arabinoxylan nanocomposite was investigated against *P. aeruginosa*, *Staph. Aureus* and *E. coli* by well-diffusion method (Jain et al., 2019). Briefly, bacterial cultures were sub-cultured on a nutrient broth for 24 h at 37 °C. Agar medium was prepared by dissolving nutrient agar (5.8 g) in water (250 mL) and autoclaved at 121 °C for 30 min. It was cooled below 50 °C and bacterial sub-cultures (1.0 mL) were added dropwise, separately in three different petri dishes and allowed to dry. Three wells of 8 mm diameter were bored with a sterile borer in the semisolid agar gel and labeled. The wells were filled with roxithromycin (100 ppm, 50 µL) a positive control, AX (500 µg mL⁻¹), and Cu-AX composite (100 µg mL⁻¹). The petri dishes were incubated for 24 h at 37 °C and zones of inhibition (ZOI) were measured against each bacterial strain. The experiment was carried out in triplicate.

2.5. Water cleaning efficacy of the synthesized copper-arabinoxylan nanocomposite

The synthesized Cu-AX composite (2.00 g) was soaked in sterile water (20 mL) and allowed to swell for about 15 min. The swollen composite was packed in a 50-mL glass burette, allowed to settle for about 15 min and the excess water was drained. The bacterial suspension (20 mL, 6×10^4 CFU mL⁻¹) was passed through the composite @ 0.5 mL min⁻¹ and the filtered water was tested for log reduction in cfu mL⁻¹ according to the formula:

$$\text{Log-reduction (CFU mL}^{-1}\text{)} = \text{CFU mL}^{-1}\text{ before filtration} - \text{CFU mL}^{-1}\text{ after filtration.}$$

In the control experiment same amount of AX (without CuNPs) was used. The copper in filtered water was determined by flame atomic absorption spectrometry. All the above experiments were performed in triplicate and the results reported as mean \pm SD. The comparison was carried out by the Student *t* test with $p < 0.05$.

2.6. Catalytic activity of copper-arabinoxylan nanocomposite

The Cu-AX composite (1.0 g) was packed in a reactor consisting of a 20-cm long stainless steel (316L) tube having 6.5 mm inner diameter. The depth of the catalyst bed was approximately 6.0 cm. The reaction mixture composed of CO₂ and H₂ in 1:3 M ratio according to the equation $\text{CO}_2 + \text{H}_2 \rightarrow \text{CH}_3\text{-OH} + \text{H}_2\text{O}$ was fed into the reactor at approximately 50 atm pressure and 400 °C. The catalyst (Cu-AX composite) was pre-treated under the flow of the gas mixture at atmospheric pressure and 250 °C for 1 h. Production of methanol was monitored by GC-MS system in splitless mode. The GC-MS system (Agilent Technologies, USA) consisted of: gas chromatograph GC7890A; mass spectrometer MS5975C with triple-axis detector; HP-5MS column (methylpolysiloxane, 30 m \times 250 µm \times 0.25 µm). The chromatographic and the mass spectrometric parameters were: helium as carrier gas with 1.0 mL min⁻¹ flowrate, 150°C injector temperature, 2 min solvent delay time, 60°C for 1 min then 10°C min⁻¹ to 200°C for 5 min as the column temperatures, 150°C MS source temperature, 280°C MSD transfer line temperature, 47 eV relative volt-

age, mass range 10–100 amu. Data were acquired and processed with the GC/MSD ChemStation® (Agilent Technologies, USA).

3. Results and discussion

3.1. Synthesis of copper-arabinoxylan nanocomposite

Synthesis of stable Cu-AX composite was successfully achieved by the method described in the section 2.2. The fully swollen AX entrapped the CuNPs and dispersed in the polysaccharide matrix as they formed giving little chance to aggregate. On the passage of electric current, Cu²⁺ ions released from the sacrificial copper anode move towards the cathode (carbon rod) where they are reduced to Cu⁰ particles and get dispersed in the AX matrix (Scheme 1). The porous structure of AX worked as a template to produce particles of uniform size. The composite thus formed was isolated by filtration and dried under vacuum and characterized.

3.2. Characterization of copper-arabinoxylan nanocomposite

3.2.1. SPR spectra

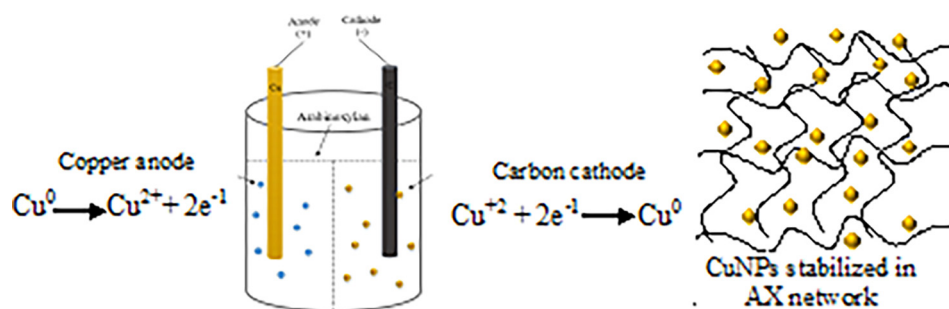
The CuNPs showed characteristic SPR absorption at 566 ± 2 nm (Fig. 1) indicating the formation of CuNPs corresponding to the particle size of 50 nm (Creighton and Eadon, 1991). The absorption band at ~ 275 nm characteristic of CuO NPs (Kumar et al., 2017b) was not observed for six days and started appearing on the seventh day. The spectrum recorded after two weeks is shown in Fig. 1b. This suggests that the synthesized CuNPs were stable for six days. There was little effect of voltage on the SPR absorption suggesting uniformity of the particles. The smooth curve in the SPR spectra suggest a spherical shape of the particles (Amendola and Meneghetti, 2009).

3.2.2. FT-IR analysis

The FT-IR spectra of both AX and the composite (Fig. 2) exhibited characteristic absorption bands of AX indicating the polymer remains intact. The peaks were assigned as: 1032 cm⁻¹ (δ C-OH), shoulders at ~ 1158 , and ~ 895 cm⁻¹ (ν_{antisym} C—O—C of the β -1,4 and glycosidic-linkages) (Barron and Rouau, 2008), 1000–1200 cm⁻¹ (ring, ν C—O—C, ν C—C, ν C—O, δ C—OH), 1247 cm⁻¹ (δ_{antisym} bridged oxygen), 1318–1373 cm⁻¹ (δ C—H), 1636 cm⁻¹ (absorbed H₂O deformation), 2893–2817 cm⁻¹ (ν O—H and methylene ν C—H), 2911–2923 cm⁻¹ (ν C—H aliphatic saturated), 3417–3449 cm⁻¹ (ν O—H). New absorption bands at ~ 1618 and ~ 1430 cm⁻¹ typical of carboxylate groups were observed in the spectrum of the composite indicating oxidation of some of the OH groups in the AX by the Cu²⁺ ions. The bands in the regions 610–632 cm⁻¹ and 519–531 cm⁻¹ (polymer backbone) were also observed. The region 800–1200 cm⁻¹ provides information about anomeric nature, glycosidic linkages, ring and alcoholic groups (Cael et al., 1974).

3.2.3. SEM analysis

SEM image of the composite is shown in Fig. 3. The spherical particles can be seen dispersed in the AX matrix. The polymeric network of hemicelluloses with available voids in their



Scheme 1 Synthesis of copper-arabinoxylan nanocomposite.

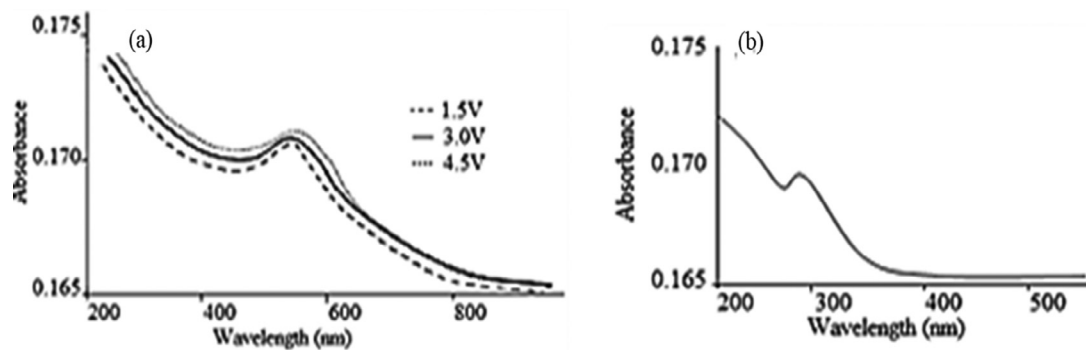


Fig. 1 (a) SPR spectra of Cu-AX nanocomposite at different experimental voltages (b) characteristic peak of CuO-NPs after two weeks indicating oxidation of CuNPs.

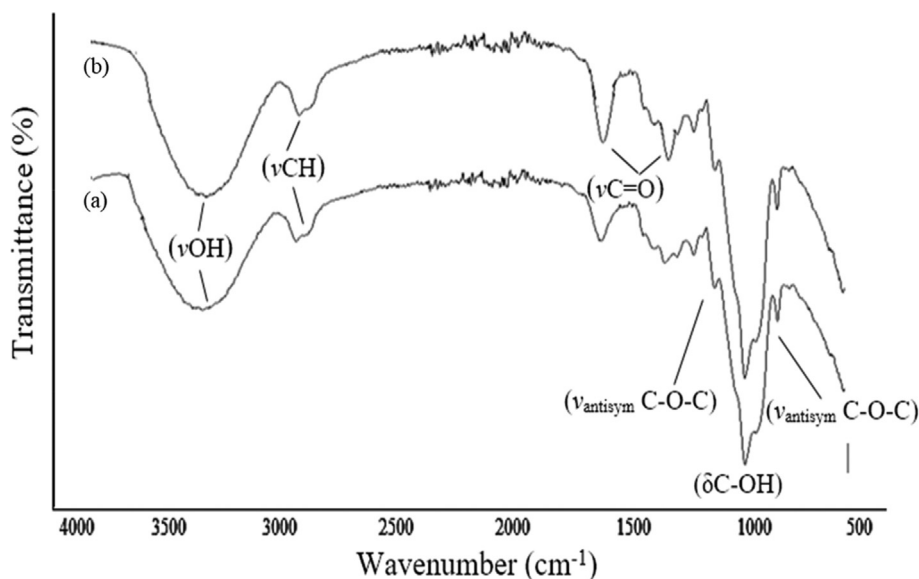


Fig. 2 FT-IR spectra of (a) AX and (b) Cu-AX nanocomposite.

structure, provides a system that prevents NPs from interaction and agglomeration thereby helping in storing NPs for longer periods of time. In the present study the synthesized particles remained stable for a period of six days, which is considerably longer period for CuNPs to remain stable in aqueous environment.

3.2.4. XRD analysis

The pXRD spectrum of the composite is shown in Fig. 4a. Sharp peaks at 2θ values 43.33, 50.8 and 74.17 corresponding to miller indices (hkl) (111), (200) and (220) planes of the crystalline particles were observed. These assignments are according to the Joint Committee on Powder Diffraction

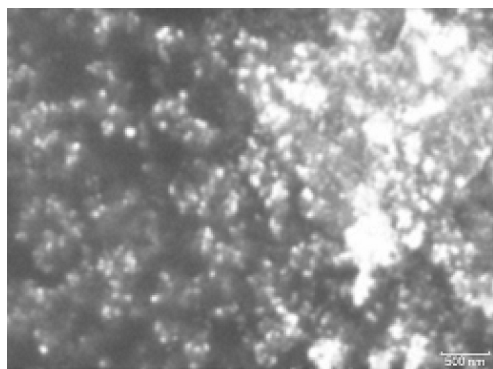


Fig. 3 SEM image of Cu-AX composite obtained at 4.5 V.

Standards (JCPDS), Card file No. 04-0836 (43.297, 50.433, 74.130). This pattern suggests a face-centered cubic structure of the particles (Liu et al., 2015; Theivasanthi and Alagar, 2011). The crystallite size as determined by Debye-Scherrer

equation (Scherrer, 1918) was found to be 50 ± 5 nm that is consistent with the SPR data presented above. The broad and weak peaks due to AX were not visible in the spectrum of the composite as AX is grossly an amorphous material.

3.2.5. DLS and zeta potential measurement

The average hydrodynamic diameter of CuNPs (Fig. 4b) measured by zeta sizer was 495.4 nm with narrow/uniform size distribution (poly dispersity index 0.484). The larger size depicted by this technique is understandable as the hydrodynamic diameter is always larger due to coating of the NPs by the polymer (Maskos and Stauber, 2011). Zeta potential can be used to predict the stability of NPs. For a stable system stabilized solely by electrostatic forces, a minimum ± 30 mV zeta potential is required (Bantz et al., 2014). Measured zeta potential (-15.3 mV) of the synthesized CuNPs (Fig. 4c) indicates that particles have a negative surface charge and are stable, which show that AX has stabilized the particles confirming its role as stabilizer and preventing aggregation.

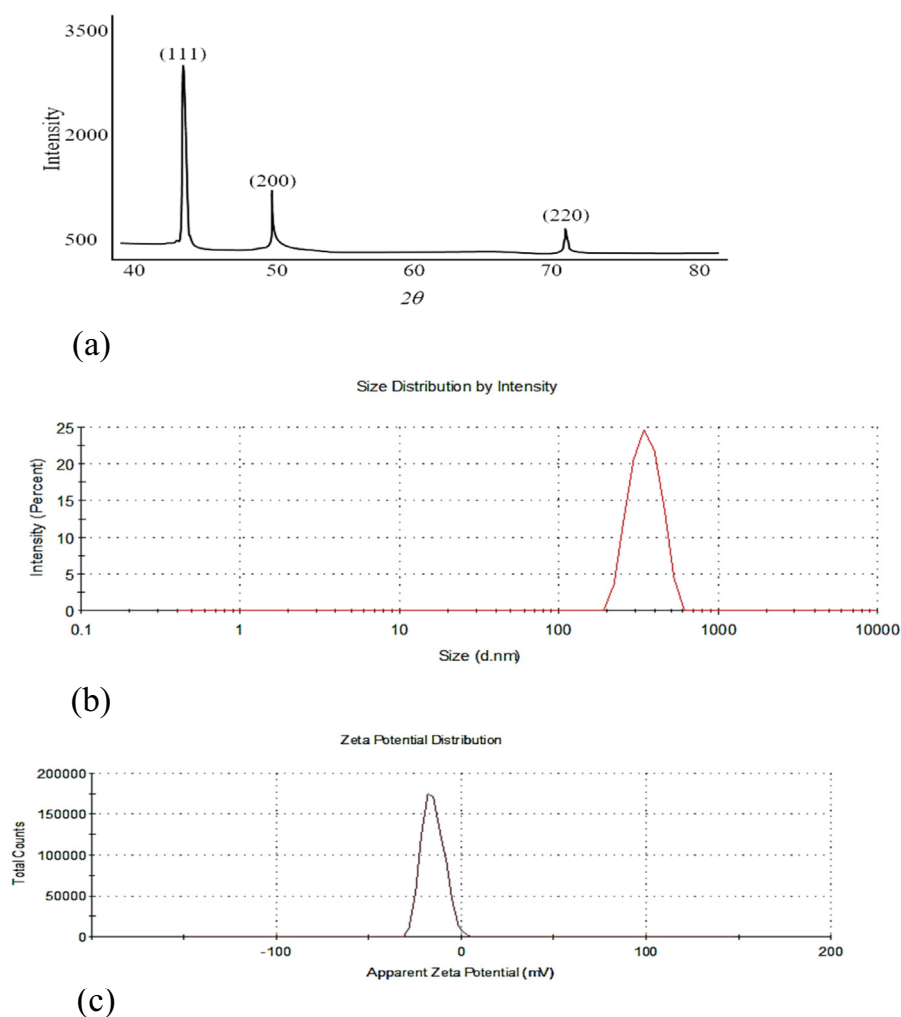


Fig. 4 (a) pXRD Spectrum, at 4.5 V, (b) Hydrodynamic diameter at 4.5 V measured by DLS technique and (c) Zeta-potential measurement at 4.5 V (indicative of negative surface charge and high stability) of Cu-AX nanocomposite.

3.3. Antimicrobial activity of copper-arabinoxylan nanocomposite

Copper-arabinoxylan nanocomposite displayed strong antimicrobial activity ($P < 0.05$) against *P. aeruginosa*, *E. coli*, and *S. aureus*, whereas the AX did not show any significant activity (Fig. 5). The particles were more sensitive toward Gram negative strains i.e., *P. aeruginosa* and *E. coli*. The results suggest that the composite can be considered as better alternative to silver NPs due to its low cost. In addition to that, copper is known to play an important role as an essential trace element in the biological system (Kalińska et al., 2019). CuNPs have been shown to have antibacterial effect on the bacterial cell functions in multiple ways, including adhesion to Gram-negative bacterial cell wall due to electrostatic interaction, having effect on protein structure in the cell membrane, denaturation of the intracellular proteins, and interaction with phosphorus and sulfur containing compounds like DNA (Baptista et al., 2018; Chatterjee et al., 2014). It has been suggested that the action of CuNPs results in 2.5 times overpro-

duction of the reactive oxygen species (Kaweeteerawat et al., 2015), lipid peroxidation, protein oxidation and DNA degradation (Mahmoodi et al., 2018).

3.4. Water cleaning efficacy of the synthesized copper arabinoxylan composite

In this experiment a log reduction of 6 was observed from 1.00 g Cu-AX nanocomposite, (containing approximately 100 mg Cu). The purified water was found to contain copper below the detection limit ($0.1 \mu\text{g L}^{-1}$). The results demonstrated approximately 50 times higher efficacy of the composite as compared with that of an AgNO_3 system (Hwang et al., 2007).

3.5. Catalytic activity of copper-arabinoxylan nanocomposite

The total ion chromatogram and the mass spectra of the converted mixture after catalytic reduction of CO_2 are shown in Fig. 6. The abundance of methanol and CO_2 in the converted mixture was found to be $\sim 85\%$ and $\sim 15\%$, respectively. The

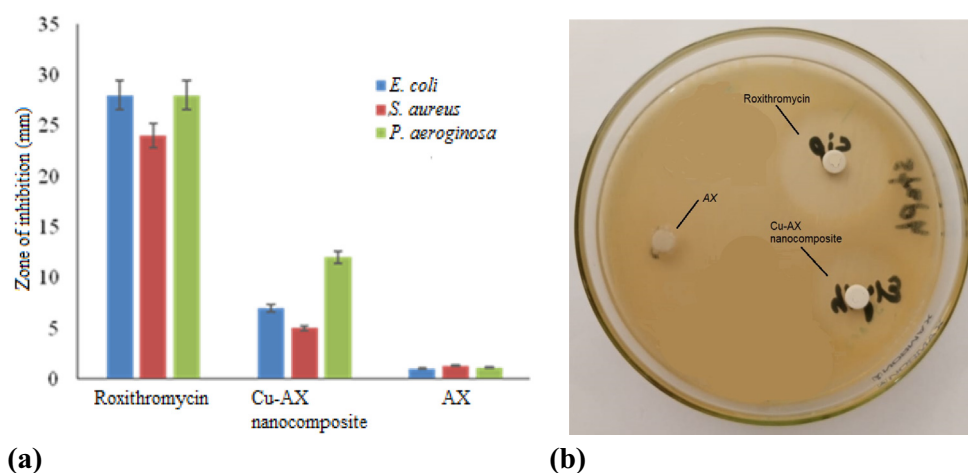


Fig. 5 A) comparative antimicrobial activity of roxithromycin (standard antibiotic), Cu-AX nanocomposite and AX (control) against Gram-positive and Gram-negative bacteria; b) A typical image showing the zone of inhibition produced by the composite against *P. aeruginosa*.

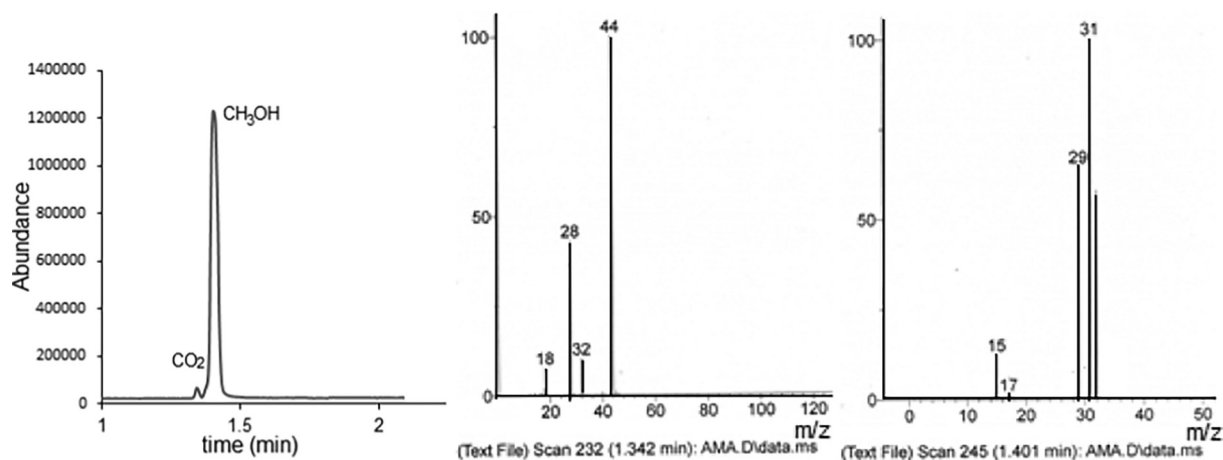


Fig. 6 The total ion chromatogram and mass spectra of the converted mixture.

conversion of CO₂ to CH₃OH in one cycle was ~ 9 %, which is comparable to that obtained with complex catalytic systems (Arakawa et al., 1992; Amenomiya 1987).

4. Conclusions

A highly stable copper-arabinoxylan nanocomposite having ~ 50 nm particle size was synthesized by electrochemical reduction by use of arabinoxylan, a natural hemicellulosic material, from the *Plantago ovata* seed husk. This method is simple, fast and economical and eliminates the use of hazardous reducing agents and provides for a clean, nontoxic and eco-friendly procedure for the synthesis of stable CuNPs at room temperature. The copper-arabinoxylan nanocomposite effectively catalyzed the reduction of CO₂ to methanol and displayed a high antimicrobial activity against *P. aeruginosa*, *E. coli*, and *S. aureus*. The composite showed great potential for cleaning infected water.

Declaration of Competing Interest

The authors declare that they have no known competing financial interests or personal relationships that could have appeared to influence the work reported in this paper.

Acknowledgments

The researchers would like to thank the Deanship of Scientific Research, Qassim University, for funding the publication of this project.

References

- Akbar, J., Iqbal, M.S., Massey, S., Masih, R., 2012. Kinetics and mechanism of thermal degradation of pentose- and hexose-based carbohydrate polymers. *Carbohydr. Polym.* 90, 1386–1393. <https://doi.org/10.1016/j.carbpol.2012.07.008>.
- Akintelu, S.A., Folorunso, A.S., Folorunso, F.A., Oyebamiji, A.K., 2020. Green synthesis of copper oxide nanoparticles for biomedical application and environmental remediation. *Heliyon*. <https://doi.org/10.1016/j.heliyon.2020.e04508>.
- Ali, L., Mumtaz, M., Ali, I., Waqee-ur-Rehman, M., Jabbar, A., 2018. Metallic Cu nanoparticles added to Cu_{0.5}Tl_{0.5}Ba₂Ca₂Cu₃O₁₀- δ superconductor. *J. Supercond. Nov. Magn.* 31, 561–567. <https://doi.org/10.1007/s10948-017-4229-8>.
- Alves, D.C., Silva, R., Voiry, D., Asefa, T., Chhowalla, M., 2015. Copper nanoparticles stabilized by reduced graphene oxide for CO₂ reduction reaction. *Mater. Renew. Sustain. Energy* 4 (2), 1–7. <https://doi.org/10.1007/s40243-015-0042-0>.
- Amendola, V., Meneghetti, M., 2009. Laser ablation synthesis in solution and size manipulation of noble metal nanoparticles. *Phys. Chem. Chem. Phys.* 11, 3805–3821. <https://doi.org/10.1039/b900654k>.
- Amenomiya, Y., 1987. Methanol synthesis from CO₂ + H₂ II. Copper-based binary and ternary catalysts. *Appl. Catal.* 30, 57–68. [https://doi.org/10.1016/S0166-9834\(00\)81011-8](https://doi.org/10.1016/S0166-9834(00)81011-8).
- Arakawa, H., Dubois, J.L., Sayama, K., 1992. Selective conversion of CO₂ to methanol by catalytic hydrogenation over promoted copper catalyst. *Energy Convers. Manag.* 33, 521–528. [https://doi.org/10.1016/0196-8904\(92\)90051-W](https://doi.org/10.1016/0196-8904(92)90051-W).
- Bantz, C., Koshkina, O., Lang, T., Galla, H.J., Kirkpatrick, C.J., Stauber, R.H., Maskos, M., 2014. The surface properties of nanoparticles determine the agglomeration state and the size of the particles under physiological conditions. *Beilstein J. Nanotechnol.* 5, 1774–1786. <https://doi.org/10.3762/bjnano.5.188>.
- Baptista, P.V., McCusker, M.P., Carvalho, A., Ferreira, D.A., Mohan, N.M., Martins, M., Fernandes, A.R., 2018. Nano-strategies to fight multidrug resistant bacteria—“A Battle of the Titans”. *Front. Microbiol.* <https://doi.org/10.3389/fmicb.2018.01441>.
- Barrière, C., Piettre, K., Latour, V., Margeat, O., Turrin, C.O., Chaudret, B., Fau, P., 2012. Ligand effects on the air stability of copper nanoparticles obtained from organometallic synthesis. *J. Mater. Chem.* 22, 2279–2285. <https://doi.org/10.1039/c2jm14963j>.
- Barron, C., Rouau, X., 2008. FTIR and Raman signatures of wheat grain peripheral tissues. *Cereal Chem.* 85, 619–625. <https://doi.org/10.1094/CCHEM-85-5-0619>.
- Begletsova, N., Selifonova, E., Chumakov, A., Al-Alwani, A., Zakharevich, A., Chernova, R., Glukhovskoy, E., 2018. Chemical synthesis of copper nanoparticles in aqueous solutions in the presence of anionic surfactant sodium dodecyl sulfate. *Colloids Surf. A Physicochem. Eng. Asp.* 552, 75–80. <https://doi.org/10.1016/j.colsurfa.2018.05.023>.
- Benavente, E., Lozano, H., Gonzalez, G., 2013. Fabrication of copper nanoparticles: advances in synthesis, morphology control, and chemical stability. *Recent Pat. Nanotechnol.* 7, 108–132. <https://doi.org/10.2174/1872210511307020002>.
- Cael, J.J., Koenig, J.L., Blackwell, J., 1974. Infrared and raman spectroscopy of carbohydrates. part IV. identification of configuration- and conformation-sensitive modes for D-glucose by normal coordinate analysis. *Carbohydr. Res.* 32, 79–91. [https://doi.org/10.1016/S0008-6215\(00\)82465-9](https://doi.org/10.1016/S0008-6215(00)82465-9).
- Chatterjee, A.K., Sarkar, R.K., Chattopadhyay, A.P., Aich, P., Chakraborty, R., Basu, T., 2012. A simple robust method for synthesis of metallic copper nanoparticles of high antibacterial potency against *E. coli*. *Nanotechnology* 23, <https://iopscience.iop.org/article/10.1088/0957-4484/23/8/085103> 085103.
- Chatterjee, A.K., Chakraborty, R., Basu, T., 2014. Mechanism of antibacterial activity of copper nanoparticles. *Nanotechnology* 25. <https://doi.org/10.1088/0957-4484/25/13/135101>.
- Chiriac, A., Dragoi, B., Ungureanu, A., Ciotonea, C., Mazilu, I., Royer, S., Mamede, A.S., Rombi, E., Ferino, I., Dumitriu, E., 2016. Facile synthesis of highly dispersed and thermally stable copper-based nanoparticles supported on SBA-15 occluded with P123 surfactant for catalytic applications. *J. Catal.* 339, 270–283. <https://doi.org/10.1016/j.jcat.2016.04.004>.
- Creighton, J.A., Eadon, D.G., 1991. Ultraviolet-visible absorption spectra of the colloidal metallic elements. *J. Chem. Soc. Faraday Trans. 87*, 3881–3891. <https://doi.org/10.1039/FT9918703881>.
- Dongare, S., Singh, N., Bhunia, H., 2021. Electrocatalytic reduction of CO₂ to useful chemicals on copper nanoparticles. *App. Surf. Sci.* 537, <https://doi.org/10.1016/j.apsusc.2020.148020> 148020.
- El Bialy, B.E., Hamouda, R.A., Eldaim, M.A.A., El Ballal, S.S., Heikal, H.S., Khalifa, H.K., Hozzein, W.N., 2020. Comparative toxicological effects of biologically and chemically synthesized copper oxide nanoparticles on mice. *Int. J. Nanomed.* 15, 3827–3842. <https://doi.org/10.2147/IJN.S241922>.
- Gawande, M.B., Goswami, A., Felpin, F.X., Asefa, T., Huang, X., Silva, R., Zou, X., Zboril, R., Varma, R.S., 2016. Cu and Cu-based nanoparticles: synthesis and applications in catalysis. *Chem. Rev.* <https://doi.org/10.1021/acs.chemrev.5b00482>.
- Guo, Y., Cao, F., Lei, X., Mang, L., Cheng, S., Song, J., 2016. Fluorescent copper nanoparticles: recent advances in synthesis and applications for sensing metal ions. *Nanoscale* 8, 4852–4863. <https://doi.org/10.1039/c6nr00145a>.
- Hwang, M.G., Katayama, H., Ohgaki, S., 2007. Inactivation of *Legionella pneumophila* and *Pseudomonas aeruginosa*: Evaluation of the bactericidal ability of silver cations. *Water Res.* 41, 4097–4104. <https://doi.org/10.1016/j.watres.2007.05.052>.
- Iqbal, M.S., Akbar, J., Saghir, S., Karim, A., Koschella, A., Heinze, T., Sher, M., 2011. Thermal studies of plant carbohydrate polymer hydrogels. *Carbohydr. Polym.* 86, 1775–1783. <https://doi.org/10.1016/j.carbpol.2011.07.020>.
- Jain, N.K., Pathak, S., Alam, M., 2019. Synthesis of copper nanoparticles by pulsed electrochemical dissolution process. *Ind. Eng. Chem. Res.* 58, 602–608. <https://doi.org/10.1021/acs.iecr.8b03146>.

- Kalińska, A., Jaworski, S., Wierzbicki, M., Gołbiewski, M., 2019. Silver and copper nanoparticles—an alternative in future mastitis treatment and prevention? *Int. J. Mol. Sci.* 20. <https://doi.org/10.3390/ijms20071672>.
- Kas, R., Kortlever, R., Milbrat, A., Koper, M.T., Mul, G., Baltrusaitis, J., 2014. Electrochemical CO₂ reduction on Cu₂O-derived copper nanoparticles: controlling the catalytic selectivity of hydrocarbons. *Phys. Chem. Chem. Phys.* 16 (24), 12194–12201. <https://doi.org/10.1039/C4CP01520G>.
- Kaweeteerawat, C., Chang, C.H., Roy, K.R., Liu, R., Li, R., Toso, D., Fischer, H., Ivask, A., Ji, Z., Zink, J.I., Zhou, Z.H., Chanfreau, G. F., Telesca, D., Cohen, Y., Holden, P.A., Nel, A.E., Godwin, H.A., 2015. Cu nanoparticles have different impacts in *Escherichia coli* and *Lactobacillus brevis* than their micro-sized and ionic analogues. *ACS Nano* 9, 7215–7225. <https://doi.org/10.1021/acsnano.5b02021>.
- Kruk, T., Gołda-Cępa, M., Szczepanowicz, K., Szyk-Warszyńska, L., Brzychczy-Włoch, M., Kotarba, A., Warszyński, P., 2019. Nanocomposite multifunctional polyelectrolyte thin films with copper nanoparticles as the antimicrobial coatings. *Colloids Surf. B Biointerfaces* 181, 112–118. <https://doi.org/10.1016/j.colsurfb.2019.05.014>.
- Kumar, R., Patel, K., Kushwaha, N., Mittal, J., 2017b. Room temperature rapid hydrogen sulfide-gas sensing using copper nanoparticles. *Sens. Lett.* 15, 584–588. <https://doi.org/10.1166/sl.2017.3854>.
- Kumar, B., Smita, K., Cumbal, L., Debut, A., Angulo, Y., 2017a. Biofabrication of copper oxide nanoparticles using Andean blackberry (*Rubus glaucus* Benth.) fruit and leaf. *J. Saudi Chem. Soc.* 21, S475–S480. <https://doi.org/10.1016/j.jscs.2015.01.009>.
- Le, M., Ren, M., Zhang, Z., Sprunger, P.T., Kurtz, R.L., Flake, J.C., 2011. Electrochemical reduction of CO₂ to CH₃OH at copper oxide surfaces. *J. Electrochem. Soc.* 158 (5), E45. <https://doi.org/10.1149/1.3561636/meta>.
- Liu, H., Wang, T., Zeng, H., 2015. CuNPs for efficient photocatalytic hydrogen evolution. *Part. Part. Syst. Charact.* 32, 869–873. <https://doi.org/10.1002/ppsc.201500059>.
- Mahmoodi, S., Elmi, A., Hallaj Nezhadi, S., 2018. Copper nanoparticles as antibacterial agents. *J. Mol. Pharm. Org. Process Res.* 06, 1–7. <https://doi.org/10.4172/2329-9053.1000140>.
- Majumdar, T.D., Singh, M., Thapa, M., Dutta, M., Mukherjee, A., Ghosh, C.K., 2019. Size-dependent antibacterial activity of copper nanoparticles against *Xanthomonas oryzae* pv. *oryzae*—a synthetic and mechanistic approach. *Colloid Interf. Sci. Commun.*, 100190. <https://doi.org/10.1016/j.colcom.2019.100190>.
- Maskos, M., Stauber, R.H., 2011. Characterization of nanoparticles in biological environments, in: *Comprehensive Biomaterials*. <https://doi.org/10.1016/b978-0-08-055294-1.00011-8>.
- Massey, S., Iqbal, M.S., Wolf, B., Mariam, I., Rao, S., 2016. Comparative drug loading and release study on some carbohydrate polymers. *Lat. Am. J. Pharm.* 35, 146–155.
- Morsi, R.E., Alsabagh, A.M., Nasr, S.A., Zaki, M.M., 2017. Multifunctional nanocomposites of chitosan, silver nanoparticles, copper nanoparticles and carbon nanotubes for water treatment: antimicrobial characteristics. *Int. J. Biol. Macromol.* 97, 264–269. <https://doi.org/10.1016/j.ijbiomac.2017.01.032>.
- Murtaza, M., Hussain, N., Ya, H., Wu, H., 2019. High purity copper nanoparticles via sonoelectrochemical approach. *Mater. Res. Express* 6. <https://doi.org/10.1088/2053-1591/ab48b6> 115058.
- Nasrollahzadeh, M., Sajadi, S.M., Rostami-Vartooni, A., Bagherzadeh, M., Safari, R., 2015. Immobilization of copper nanoparticles on perlite: green synthesis, characterization and catalytic activity on aqueous reduction of 4-nitrophenol. *J. Mol. Catal. A: Chem.* 400, 22–30. <https://doi.org/10.1016/j.molcata.2015.01.032>.
- Numaga, N., Hayashi, H., Smith, R.L., 2020. Supercritical hydrothermal synthesis of polyacrylic acid-capped copper nanoparticles and their feasibility as conductive nanoinks. *J. Electron. Mater.* 49, 5681–5686. <https://doi.org/10.1007/s11664-020-08370-w>.
- Pant, J., Goudie, M.J., Hopkins, S.P., Brisbois, E.J., Handa, H., 2017. Tunable nitric oxide release from S-Nitroso-N-acetylpenicillamine via catalytic copper nanoparticles for biomedical applications. *ACS Appl. Mater. Interfaces* 9, 15254–15264. <https://doi.org/10.1021/acsmi.7b01408>.
- Ponce, A.A., Klabunde, K.J., 2005. Chemical and catalytic activity of copper nanoparticles prepared via metal vapor synthesis. *J. Mol. Catal. A: Chem.* 225 (1), 1–6. <https://doi.org/10.1016/j.molcata.2004.08.019>.
- Rakhmetova, A. A., Alekseeva, T. P., Bogoslovskaya, O. A., Leipunskii, I. O., Ol'khovskaya, I. P., Zhigach, A. N., Glushchenko, N. N., 2010. Wound healing properties of copper nanoparticles as a function of physicochemical parameters. *Nanotechnologies in Russia* 5, 271–276. <https://doi.org/10.1134/S199507801003016X>.
- Scherrer, P., 1912. Bestimmung der inneren Struktur und der Größe von Kolloidteilchen mittels Röntgenstrahlen. *Kolloidchemie Ein Lehrbuch*, 387–409. https://doi.org/10.1007/978-3-662-33915-2_7.
- Scherrer, P., 1918. Bestimmung der Größe und der inneren Struktur von Kolloidteilchen mittels Röntgenstrahlen. *Nachrichten von der Gesellschaft der Wissenschaften zu Göttingen. Math. Klasse* 1918, 98–100.
- Theivasanthi, T., Alagar, M., 2011. Nano sized copper particles by electrolytic synthesis and characterizations. *Int. J. Phys. Sci.* <https://doi.org/10.5897/IJPS10.116>.